A MATHEMATICAL DUCTILE EROSION MODEL TO CHARACTERIZE ASH PARTICLES EROSION ON BOILER GRADE STEEL SURFACES

S.K.Das[1*] ,K.M.Godiwalla, Shubha Hegde
S.P.Mehrotra, and P.K.Dey

National Metallurgical Laboratory
(Council of Scientific & Industrial Research)
Jamshedpur 831 007
*Contact Email: skd@nmlindia.org

KEYWORDS**:** Mathematical model, erosion rate, boiler components, fly ash impingement, tensile properties, steel grades

ABSTRACT

Fly ash particles entrained in the flue gas from boiler furnaces in coal-fired power stations can cause serious erosive wear on steel surfaces along the flow path. Such erosion can reduce significantly the operational life of the boiler components. A fundamentally-derived mathematical model embodying the mechanisms of erosion involving cutting wear, plastic deformation wear and effect of temperature on erosion behaviour, has been developed to predict erosion rates on the coal fired boiler components such as boiler tubes, economizer and air-preheater assemblies at room and elevated temperature. Various grades of steels, commonly used in the fabrication of boiler components and published data pertaining boiler fly ash has been used for modelling the process. The model incorporates the tensile properties of the target metal surface at room and elevated temperatures, as well as the characteristics of the ash particle dynamics in the form of impingement angle, impingement velocity and composition of the ash particle in terms of the silica content. The mathematical model has been implemented in an user-interactive in-house computer code, (**EROSIM–1**) to predict the erosion rates at room and elevated temperature for various grades of steel normally used in boiler components. The model predictions have been found to be in good agreement with the published data. The model will be calibrated in future with the plant and experimental data generated from a high temperature air-jet erosion testing facility. It is hoped that the calibrated model will be useful to the power plant industry for erosion analysis of boiler components.

1. INTRODUCTION

In coal-fired power stations, about 20% of the ash produced in the boilers is deposited on the boiler walls , economizers, air-heaters and super-heater tubes. This deposited ash is subsequently discharged as slag and clinker during the soot blowing process. The rest of the ash is entrained in the stream of flue gas leaving the boiler. The ash particles collide with the surfaces of the boiler steel components and the material is eroded from the surface. In advanced stages of erosion, the components get perforated. The components may fail once they lose their structural integrity. Such erosion, together with the processes of blocking, fouling and corrosion, shortens the service life of the boiler components. Once this happens, the power station unit has to be shut down in order to replace the damaged components. The resulting penalty is not only the cost of replacing the components but also the cost of stoppage of power production. It is desirable, therefore, to be able to predict the rate of erosion of the coal fired boiler components in order to plan systematically for the maintenance or replacement of these components to avoid forced outages. Figure.1 is a schematic of a coal fired boiler assembly.

The problem of solid particle erosion has been addressed by various investigators and but it has remained confined to room temperature investigations. Many parameters are now known to influence erosion behaviour. The magnitude and direction of an ash particle's impact velocity relative to the target metal surface constitute essential data needed for evaluating erosion of the surface due to particle impact. The magnitude and direction of a particle's rebounding velocity depend upon the conditions at impact and the

particular particle-surface material combination. The restitution behaviour is a measure of the momentum lost by the particle at impact as such, and it corresponds to the work done on the target surface which in turn, is a measure of the extent of erosion suffered by the material of the target surface. The velocity coefficients of restitution depend upon the hardness of the target material, the density of the particle and the velocity at which the particle strikes the target surface. Grant and Tabakoff [1] developed empirical correlations of the velocity restitution coefficients for sand particles impacting 410 stainless steel. They used correlations in simulating the particle rebounding conditions solid particles ingested into rotating machinery. Meng and Ludema [2] have reviewed some of the erosion models that have been developed since Finnie [3] proposed the first analytical erosion model. These models include a variety of parameters that influence the amount of material eroded from a target surface and the mechanism of erosion. Finnie [3] calculated the erosion of surfaces by solid particles by using the following derived equations

$$\varepsilon_{vp} = \frac{mV^2}{P\psi k}\left(\sin(2\alpha) - \frac{6}{k}\sin^2\alpha\right) for \tan\alpha \leq \frac{k}{6}$$

(1)

$$\varepsilon_{vp} = \frac{mV^2}{P\psi k}\frac{k\cos^2\alpha}{6} for \tan\alpha \geq \frac{k}{6}$$

(2)

where ε_{vp} is the volume of material removed by a single abrasive grain of particle, m is mass of single particle, V is velocity of particle, P is constant of plastic flow stress, ψ is the ratio of depth of contact to the depth of cut, k is thermal conductivity of the target and α is the impact angle. Subsequently Bitter [4,5] calculated the total erosion rate which is the sum of erosion due to cutting mechanisms and deformation mechanism with out the effect of temperature by the following derived equations:

$\varepsilon_{vT}=\varepsilon_{vD} + \varepsilon_{vC}$ (3)

$$\varepsilon_{vD} = \frac{1}{2}\frac{M(V\sin\alpha - K)^2}{\delta}$$

(4)

$\varepsilon_{vC}1 =$

$$\frac{2MV(V\sin\alpha - K)^2}{(V\sin\alpha)^{1/2}}\left(V\cos\alpha - \frac{C(V\sin\alpha - K)^2}{(V\sin\alpha)^{1/2}}\chi\right) for \alpha \geq \alpha_{p0}$$

(5)

$$\varepsilon_{vC2} = \frac{\frac{1}{2}M[V^2\cos^2\alpha - K_1(V\sin\alpha - K)^{3/2}]}{\chi} for \alpha \leq \alpha_{p0}$$

(6)

where ε_{vT} is total volume erosion rate, ε_{vD} is volume of material removed by deformation mechanism, ε_{vC} is

the volume of material removed by cutting mechanisms , M is total mass of impinging particle, K is velocity component normal to surface below which no erosion takes place in certain hard materials, K_1 is proportionality constant and C is constant.

The experimental and computational investigations carried out by Jun and Tabakoff [6] and Fan et al. [7] have contributed to the understanding the mechanisms of erosion, but the detailed processes leading to material removal are still poorly understood. This means that with a few exceptions, good models for predicting the behaviour of materials during erosion rate are still not readily available. Temperature is another important influencing factor in the rate of erosion. The high temperature erosion behaviour is very complex owing to the variations in materials properties, degree of oxidation etc. Tilly [8] reported test results of various materials up to 600^0C and observed varying tendencies depending on materials. Recently the development of coal conversion and utilisation technology has accelerated the need for greater elucidation of the particle erosion behaviour, particularly at elevated temperatures. It has been observed that erosion rate of steels impacted at low angles increase as the temperature of the steel is increased. Also, it is observed that rates of erosion vary depending on the type and composition of steel.

2. MATHEMATICAL EROSION MODEL

Erosion is a process in which material is removed from the layers of a surface impacted by a stream of abrasive particles. Erosion is localised in a small volume of the target material that is eventually removed. The magnitude of the wear is quantified by the volume or mass of the material that is removed by the action of the impacting particles. It is perceived that there are three important phenomena by which metal can be removed at elevated temperature.

1. Removal of material due to cutting wear
2. Removal of material due to repeated plastic deformation.
3. Effect of temperature on the tensile properties of the material

The first two phenomena are applicable for erosion at room temperature where effect of temperature may be ignored. The relative contribution of the first two phenomena is difficult to predict due to many process and material parameters that are involved. The effect of temperature on the erosion behaviour of boiler components is of practical importance and an attempt was made to functionally correlate the tensile properties of these materials at elevated temperatures, which has been incorporated in the model. In the present model, the process and materials parameters that are considered for the prediction of erosion rate in the boiler components are the followings:

1.) Ash particle velocity, 2.)Ash particle impingement angle, 3) Mass fraction of silica contained in the ash sample, 4)Average density of ash particles, 5)Density

of the steel component , 6)Yield stress of the steel component, 7)Temperature of the steel component

Six steel compositions which have been considered in the present modelling study These are: Carbon steel, 1.25 Cr-1Mo-V steel, 2.25Cr-1Mo steel, 12Cr-1Mo-V steel, 304 steel and Alloy 800 steel. The compositions of these steels (target material) are given in Table-I and composition of a typical boiler fly ash particle (erodent) is shown in Table II.

2.1 Cutting Wear

The ash particle that strike the surface at an acute angle and at a velocity greater than the critical velocity needed for the penetration of the material's surface do remove some material , in a process similar to the cutting action of a machine tool. At the impact location the particle loses a fraction of its kinetic energy to the target material in the form of heat and energy for deformation of the surface. Very high levels of shear strain may be induced in the material at the impact location. When the shear strain exceeds the elastic strain limit of the target material, the particle penetrates the surface of the material and ploughs along the surface, removing material in a process similar to the machining action of a cutting tool.

During wear process, it is assumed that the stresses acting at the contact point are constant. The ash particle penetrating the surface of the material has to overcome the material's resistance to deformation. The equation of motion for the depth of penetration, h, of a particle of mass m_p and diameter d_p, as it penetrates through the surface of a material, developed by Kragelsky et al. [9], has been applied in the present formulation in the form of following differential equation;

$$m_p \frac{d^2 h}{dt^2} = -\pi \frac{d_p}{2} hc\sigma_y \qquad (7)$$

where t is the time, σ_y the yield stress of the target material, and C is a particle shape factor equal to 3 for a sphere. The negative sign in Eq. (7) accounts for the fact that the material resists the penetrating action of the impacting particle. The mass, m_p, for a spherical particle is derived from the following simple relationship:

$$m_p = \frac{1}{6} \rho_p \pi d_p^3 \qquad (8)$$

Substituting for the mass of the spherical particle, Eq. (7) can then be written as follows:

$$\frac{d^2 h}{dt^2} = -\frac{9\sigma_y h}{\rho_p d_p^2} \qquad (9)$$

When a particle strikes a surface with a velocity V and at an angle of incidence β, the initial rate at which the particle penetrates into the material is equal to the normal component of the impact velocity. Eq. (9), is integrated using the the initial conditions that at *t=0, (dh/dt) = Vsinβ,* and the following equation is obtained:

$$\frac{dh}{dt} = \pm\sqrt{V^2 \sin^2 \beta - \frac{9\sigma_y h^2}{\rho_p d_p^2}}$$

$$(10)$$

The physical significance of plus sign in Eq. (10) corresponds to an increase in the depth of penetration and the minus sign corresponds to a decrease in the depth of penetration. The maximum depth of penetration, h_{max}, occurs when (dh/dt) $=0$, and is given by the following equation:

$$h^3_{max} = \frac{d_p^3}{3^3} V^3 \sin^3 \beta \left(\frac{\rho_p}{\rho_y} \right)^{3/2} \qquad (11)$$

Since the volume of material that is cut away from the target surface by the impacting particle is proportional to h^3_{max}, the mass of material removed by a single particle will also be proportional to the value of h^3_{max} derived in the Eq. (11). The mass of material eroded 'm' by a single impacting particle is given by the following equation:

$$m = K_c \rho_m h^3_{max} = \frac{K_c \rho_m \rho_p^{3/2} d_p^3 V^3 \sin^3 \beta}{3^3 \sigma_y^{3/2}}$$

$$(12)$$

here K_c is a constant and ρ_m the density of target material. The erosion rate due to cutting wear, defined as the ratio of the mass of the material eroded from the target surface to mass of the impacting particle, is given by the following equation:

$$\varepsilon_c = \frac{m}{m_p} = \frac{K_c \rho_m \rho_p^{3/2} d_p^3 V^3 \sin^3 \beta}{3^3 \sigma_y^{3/2} \left(\pi \rho_p \frac{d_p^3}{6} \right)}$$

$$= \frac{K_1 \rho_m \rho_p^{1/2} V^3 \sin^3 \beta}{\sigma_y^{3/2}} \qquad (13)$$

where K_1 is a constant.

2.2 Plastic Deformation Wear

During particle impact, the loss of material from an eroding surface may occur by a combined extrusion-forging mechanism. Platelets are initially extruded from shallow craters made by the impacting particle. Once formed, the platelets are forged into a strained condition, in which they are vulnerable to being knocked off the surface in one or several pieces. Because of the high strain rates, adiabatic shear heating occurs in the surface region immediate to the impact site. Beneath the immediate surface region, a work hardened zone forms, since the kinetic energy of the impacting particles is enough to result in a considerably greater force being imparted to the metal than is required to generate platelets at the surface.

When the surface has been completely converted to platelets and craters and the work-hardened zone has reached its stable hardness and thickness, steady state erosion begins. The reason that the steady state erosion rate is the highest rate is that the subsurface cold-worked zone acts as an anvil, thereby increasing the efficiency of the impacting particles to extrude-forge platelets in the now highly strained, and most deformable, surface region. This cross section of material conditions will move down through the metal as erosion loss occurs. In the platelet mechanism of erosion, there is a localised sequential extrusion and forging of metal in a ductile manner, leading to removal of the micro segments thus formed.

During plastic deformation, the normal component of the particle's kinetic energy is used to extrude-forge the material. The normal component of the kinetic energy of the particle is given by the following equation:

$$E_1 = \frac{1}{2} \frac{\pi d_p^3}{6} \rho_p V^2 \sin^2 \beta = \frac{\pi}{12} \rho_p d_p^3 V^2 \sin^2 \beta \tag{14}$$

where d_p and ρ_p are the particle diameter and density, respectively, and V and β the particle incident velocity and angle, respectively.

The work done by the normal force N of the indenting particle in a direction h normal to the surface from the time of surface contact until penetration stops at a depth h_{max} is given by the

$$E_2 = \int_0^{h_{max}} N dh \tag{15}$$

Sheldon and Kanhere [11] formulated the following equation, relating the force N and the diameter δ of the crater formed in the indented surface

N=aδ^n (16)

where, constants, n and a, are given as follows :

n = 2.0 and

$$a = \frac{1}{4} \pi H_V$$

H_V is Vickers hardness number of the target surface eroded by particle impingement. Substituting Eq. (16) into Eq. (15) yields the following equation:

$$E_2 = \frac{\pi H_V}{4} \int_0^{h_{max}} \delta^2 dh \tag{17}$$

The depth of penetration, h, is related to the instantaneous crater diameter δ and the particle diameter d_p by the following equation:

$$h = \frac{1}{2}(d_p - (d_p^2 - \delta^2)^{\frac{1}{2}}) \tag{18}$$

Eq. (18) is used to express the particle's depth of penetration in terms of the instantaneous crater diameter. Eq. (17) is then integrated with respect to the

instantaneous crater diameter. Equating the work done during indention to the normal component of kinetic energy given in Eq. (14), the following equation is obtained:

$$\frac{\pi}{12} d_p^3 \rho_p V^2 \sin^2 \beta$$

$$= \frac{\pi H_V}{8} \int_0^{h_{max}} \frac{\delta^2 d\delta}{(d_p^2 - \delta^2)^{1/2}} \tag{19}$$

The integral in Eq. (19), is evaluated and the maximum depth of penetration is derived as:

$$\tag{20}$$

$$h_{max}^3 = \frac{d_p^3 V^3 \sin^3 \beta \rho_p^{3/2}}{H_V^{3/2}}$$

Since the dimensions of the crater formed by the impacting particle are all proportional to h_{max}^3, and since the amount of material removed is nearly the full crater size, the mass of material removed by a single particle is proportional to the value of h_{max}^3 derived in Eq. (20). The mass of material removed by a single particle is given by the following equation:

$$m = K_p \rho_m h_{max}^3 = K_p \rho_m \rho_p^{1/2} \frac{d_p^3 V^3 \sin^3 \beta}{H_V^{3/2}} \tag{21}$$

where K_p is a constant and ρ_m is the density of the target material. The erosion rate, ε_p, due to plastic deformation is given by the following equation:

$$\varepsilon_p = \frac{m}{m_p} = \frac{K_p \rho_m \rho_p^{1/2} d_p^3 V^3 \sin^3 \beta}{H_V^{3/2} (\rho_p \pi d_p^3 / 6)} = \tag{22}$$

$$\frac{K_2 \rho_m \rho_p^{1/2} V^3 \sin^3 \beta}{H_V^{3/2}}$$

where K_2 is a constant.

2.3. Overall Erosion rate and effect of Temperature

The erosion by fly ash of the boiler components consists of the wear due to the cutting mechanism plus the wear due to the plastic deformation mechanism. However, it is difficult to predict accurately the proportions contributed by each of the two mechanisms to the overall material loss. Eq. (22), which was derived for the plastic deformation wear, is similar to Eq. (19) for the cutting wear. The yield stress of a metal can be related to the metal's hardness. Tabor [12] gives the following relationship between the yield stress and Vickers hardness number:

H_V = 2.7σ_y

$$\tag{23}$$

The overall erosion rate, combining the cutting and plastic deformation wear mechanisms, is then given by the following equation:

$$\varepsilon = \frac{K_3 \rho_m \rho_p^{1/2} V^3 \sin^3 \beta}{\sigma_y^{3/2}} \tag{24}$$

where K_3 is a constant which is documented in the literature [2,3,11,12,13]. From the investigations carried out by various investigators [12,13,14,15], the erosion rate due to solid particle impact depends upon the particle impingement angle and the characteristics of the particle-wall combination for modelling erosion by fly ash of ductile metal surfaces. The constant K_3 in Eq. (24) may be replaced by the particle erosion index; the expression for the overall erosion rate is then given by Eq.(25):

$$\varepsilon = \frac{K_e I_e(x)\rho_m \rho_p^{1/2} V^3 \sin^3 \beta}{\sigma_y^{3/2}} \quad (25)$$

where K_e is a constant, x the mass fraction of silica contained in the ash sample, and I_e the erosion index of the ash, which relates the variation of the erosion rate to the silica content.

The temperature effect can be introduced on the basis of the observation that the erosion rate at acute impingement angle increase significantly with temperature suggesting that steel tends to show a behaviour more typical of a ductile material as the temperature is increased. The yield stress (Kgf/mm^2) and temperature (C) functionality has been derived through a polynomial approximation for various grades of steel on the basis of the available tensile property data at elevated temperature [16]. The following expressions have been generated.

- Carbon Steel

$$\sigma_y = 2*10^{-5}*T^2 - 0.0353*T + 30.871 \quad (26)$$

- Cr-1Mo-V steel

$$\sigma_y = -2*10^{-5}*T^2 - 0.0278*T + 48.703 \quad (27)$$

- 2.25Cr-1Mo steel

$$\sigma_y = -5*10^{-8}*T^3 + 10^{-5}*T^2 - 0.0133*T + 33.324 \quad (28)$$

- 12Cr-1Mo-V steel

$$\sigma_y = -5*10^{-7}*T^3 + 0.0005*T^2 - 0.1379*T + 59.169 \quad (29)$$

- 304 steel

$$\sigma_y = -2*10^{-8}*T^3 + 6*10^{-5}*T^2 - 0.0485*T + 28.179 \quad (30)$$

- Alloy (Incoloy) 800

$$\sigma_y = -5*10^{-8}*T^3 + 7*10^{-5}*T^2 - 0.036*T + 20.858 \quad (31)$$

3. NUMERICAL IMPLEMENTATION

The model has been implemented in a user-interactive computer code (**EROSIM-1**) which embodies the solid particle erosion mechanism due to cutting wear and repeated plastic deformation. The overall erosion is estimated from the contributions of both the mechanisms of wear. The code predicts the erosion rate in terms of the weight (mg) of the target material removed per weight (kg) of the impacting fly ash particle as a function of impact velocity, impact angle, density and silica content of the ash particle and density and yield stress of the target material. The erosion behaviour at elevated temperature has been incorporated through the derived functionality of the tensile property (yield stress) with temperature using Eq. (26) – (31) for appropriate modification of yield strength.

4. RESULTS AND DISCUSSION

Some typical results of model predictions are presented in this Figs. 2 and 3 show the variation of erosion rate with velocity, at impingement angle of 30^0 and room temperature for Carbon steel and 1.25Cr-1Mo-V steel respectively . It may be observed that there is an increase in erosion rate with increasing impacting particle velocity for both cases. Figs 4,5 & 6 show the variation of erosion rate with temperature for Carbon steel, 1.25Cr-1Mo-V steel and alloy 800 steel respectively. A tendency for the erosion rate to increase with temperature was observed for all steels. Thus, it may be concluded that the erosion rate of steels impacted at low angles definitely increases as the temperature is increased. Also, the rates of erosion were significantly different depending on the type of the steel. Fig.7 and 8 show the erosion rate as a function of particle impact angle for carbon steel and 1.25Cr-1Mo-V steel respectively at room temperature (30 C) and at elevated temperatures of 300C and 600 C . It is observed that for all temperature level, for low impingement angle, the erosion rate increased with an increase in the impingement angle until a maximum value was reached at an angle between 25^0 and 30^0 . Thereafter, the erosion rate fell off rapidly from a peak value . Fig. 9 & 10 show the erosion rate as a function of particle impact velocity for carbon steel and 1.25Cr-1Mo-V steel respectively at room temperature (30 C) and at elevated temperatures of 300C and 600 C . It is observed that at elevated temperatures also, the erosion rate is monotonically increased with increase in the particle impingement velocity .The model based code (EROSIM 1) has been validated as an efficient predictive tool with the published information [14,15,16] for the erosion of boiler components.

5.CONCLUSION

A model to predict the erosion rate for fly ash particle impingement on boiler component surfaces has been developed and the variation of erosion rate with various parameters has been determined and found to

be in good agreement with published experimental data. It is found from this modelling study that the erosion rate on steel surface subjected to a stream of impingement angle, with the maximum erosion rate occurring at an impingement angle of about 30^0. There after the erosion rate decreases with a further increase in impingement angle. The temperature effect was observed such that, as the temperature increased, the erosion rate at low impingement angles increased significantly but at high impingement angle angles it did not change significantly. All the steel grades showed an increase in erosion rate with temperature. the variation of

fly ash particles varies with the particle impingement angle. For low values of impingement angle, the erosion rate increase with an increase in the erosion rate shows a monotonic rise with ash particle impact velocity. The code has been validated with the published information. The ash particle impact angle, which is one of the important parameters influencing the erosion rate, requires further study. The influences of the shape and rotation angle of the ash particles on the erosion rate also needs further investigation using mathematical models.

REFERENCES

[1]. G. Grant, W. Tabakoff, Erosion prediction in turbomachinery resulting from environmental solid particle, J.Aircraft 1975, vol.12, pp.471-478

[2]. H.C. Meng, K.C. Ludema, Wear models and predictive equations: their form and content, Wear 1995, vol. 181-183 , pp.443-457.

[3]. I. Finnie, Erosion of surfaces by solid particles, Wear 1960, vol. 142 , pp. 87-103

[4]. J.G.A. Bitter, A study of erosion phenomenon, Part 1, Wear 1963, vol. 6 , pp. 5-21.
[5]. J.G.A. Bitter, A study of erosion phenomenon, Part 2, Wear 1963, vol. 6 , pp. 169-191.
[6]. Y.D. Jun, W. Tabakoff, Numerical simulation of a dilute particulate flow (laminar) over tube banks, Trans. ASME: J.Fluids Eng. 1994, vol. 116 , pp. 770-777.
[7]. J. Fan, D. Zhou, K. Cen, J. Jin., Numerical prediction of tube row erosion by coal ash impaction, Chem. Eng. Commun. 1990, vol. 95 pp. 75-88.
[8]. G.P. Tilly, Wear, 1969,vol. 14 , pp.63.

[9]. I.V. Kragelsky, M.N. Dobychin, V.S. Komalov, Friction and Wear Calculation Methods, Pergamon Press, 1982

[10]. G.I. Sheldon, A. Kanhere, An investigation of impingement erosion using single particles, Wear 1972, vol. 21, pp. 195-209.
[11].D. Tabor, The hardness of Metals, Oxford University Press, 1951.
[12]. Y.D. Jun, W. Tabakoff, Numerical simulation of a dilute particulate flow (laminar) over tube banks, Trans. ASME: J.Fluids Eng. 1994, vol. 116 , pp. 770-777.
[13]. J. Fan, D. Zhou, K. Cen, J. Jin, Numerical prediction of tube row erosion by coal ash impaction, Chem. Eng. Commun. 1990, vol. 95 pp. 75-88.
[14]. G.I. Sheldon, A. Kanhere, An investigation of impingement erosion using single particles, Wear 1972, vol. 21, pp. 195-209.
[15].G.L. Sheldon, J. Maji, C.T. Crowe, Erosion of a tube by gas-particle flow, Trans. ASME: J. Eng. Mater. Technol. 1977, vol .99 , pp. 138-142.
[16].Y.Shida and H.Fujikawa, Particle erosion behaviour of boiler tube materials at elevated temperature, Wear, 1985,vol 103 , pp 281-296

Steel	Amount (wt%) of the following metals						
	C	Si	Mn	Ni	Cr	Mo	V
C Steel	0.22	0.28	0.65				
1.25Cr-1Mo-V	0.13	0.25	0.55		1.20	0.95	0.30
2.25Cr-1Mo	0.10	0.34	0.44		2.20	0.98	
12Cr-1Mo-V	0.19	0.33	0.59		11.40	0.87	0.28
304	0.08	0.62	1.68	10.25	18.50		
Alloy 800	0.07	0.51	1.13	32.85	20.85		

Table –I Chemical composition of various grades of steel

Compound occurring in ash	% composition
Silica (SiO_2)	55.20
Aluminium oxide (Al_2O_3)	30.80
Iron oxide (Fe_2O_3)	3.67
Titanium oxide(TiO_2)	1.61
Phosphorous pentoxide (P_2O_5)	0.35
Calcium oxide (CaO)	5.01
Magnesium oxide (MgO)	1.40
Sodium oxide(Na_2O)	0.20
Potassium oxide(K_2O)	0.73
Sulphur(S)	0.20
Manganese oxide (MnO)	0.03

Table II Chemical (elemental) composition of a typical boiler fly ash sample
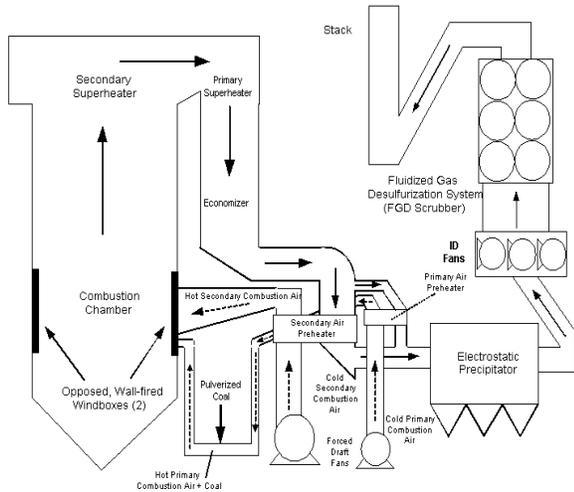
Figure.1 Coal- fired Boiler assembly
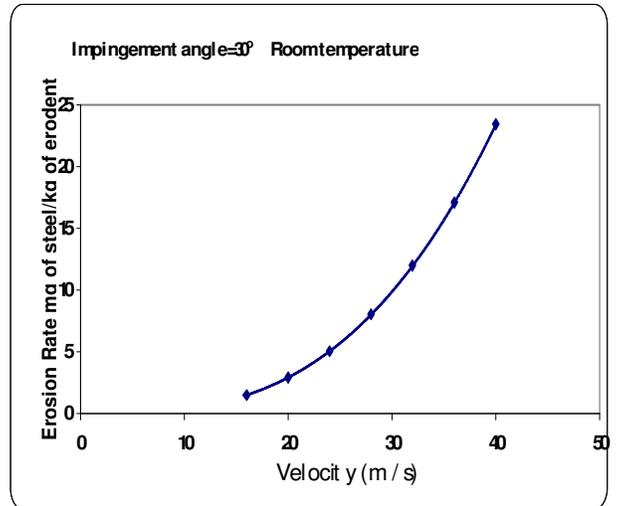
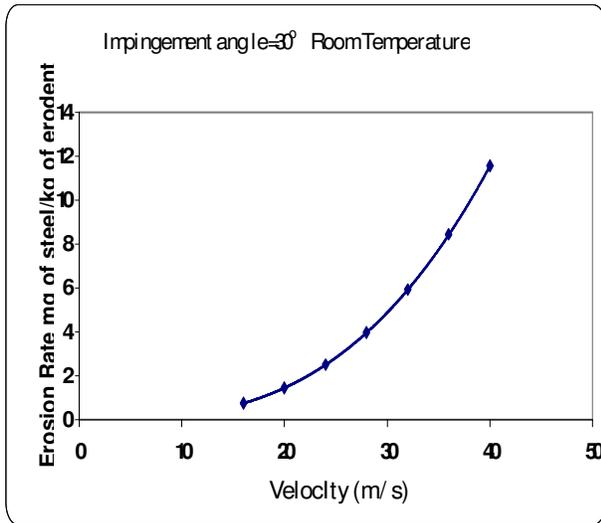**Figure 2.** Variation of erosion rate with impingement velocity (Carbon steel)

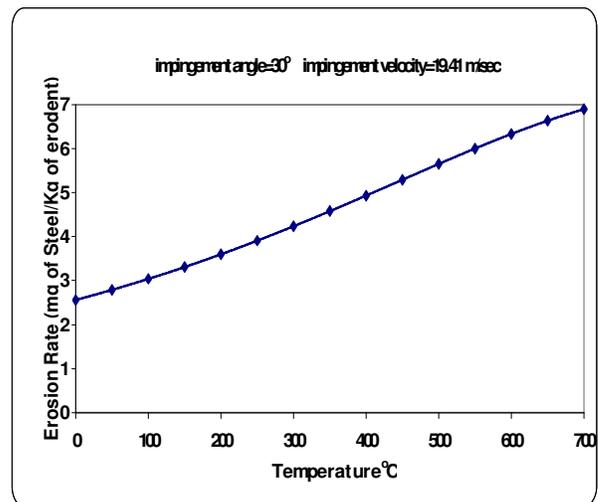**Figure. 3** Variation of erosion rate with impingement velocity (1.25 Cr-1Mo-V Steel)

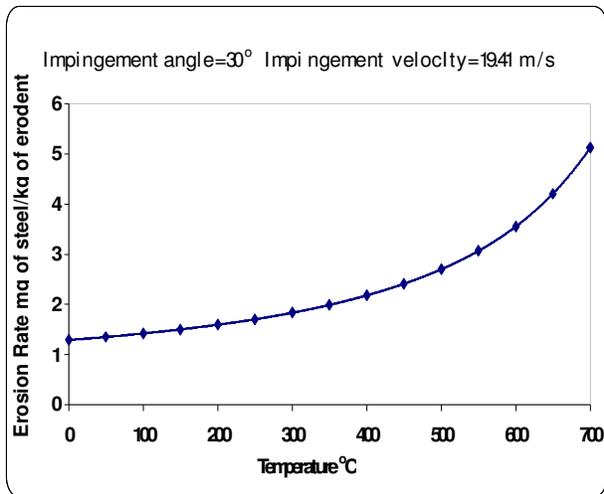**Figure. 4** Variation of erosion rate with temperature of target material (Carbon Steel)

196

Impingement angle=30° Impingement velocity=19.41 m/s

Figure. 5 Variation of erosion rate with temperature of target material (1.25Cr-1Mo-V Steel)

Impingement angle=30° Impingement velocity=19.41m/sec
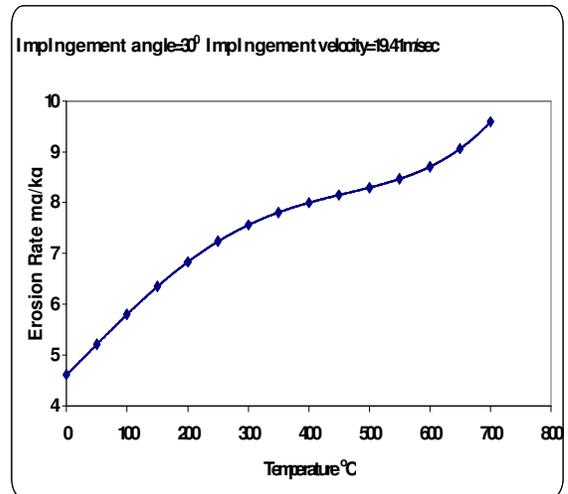
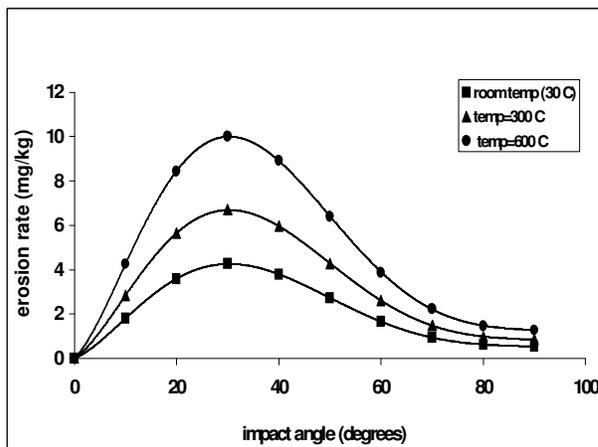**Figure. 6** Variation of erosion rate with temperature of target material (alloy 800 Steel)

Figure 7 Variation of erosion rate with impingement angle at room temperature, and elevated temperatures at 300 C and 600 C (Carbon steel)
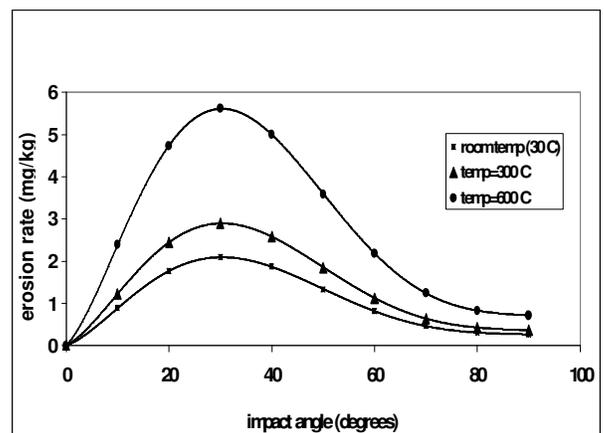

Figure.8. Variation of erosion rate with impingement angle at room temperature, and elevated temperatures at 300C and 600 C (1.25Cr-1Mo-V Steel)
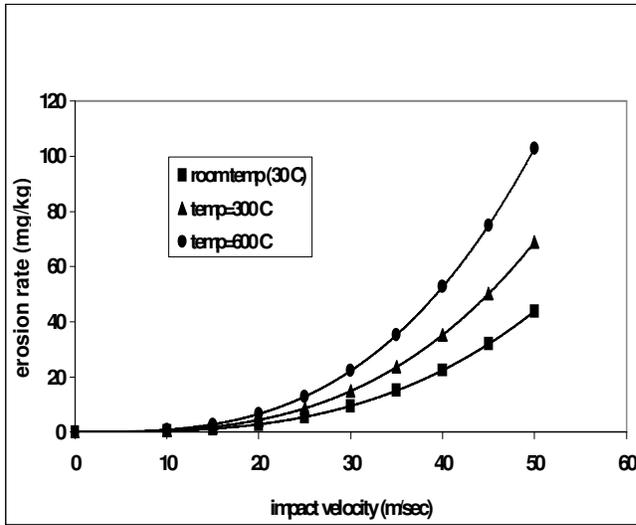
197

Figure. 9 Variation of erosion rate with impact velocity at room temperature, and elevated temperatures at 300 C and 600 C (Carbon steel)
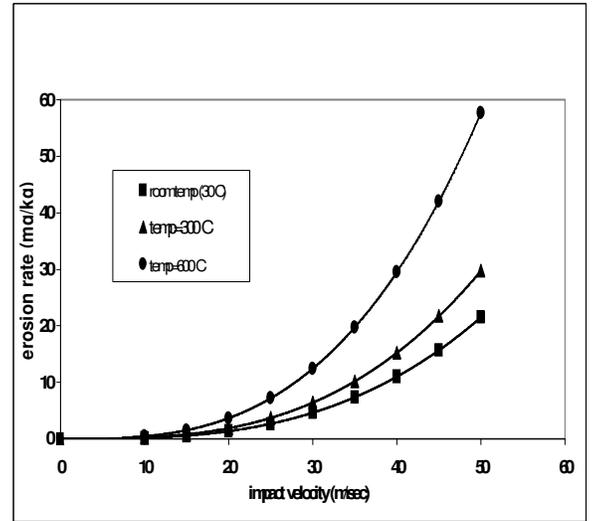

Figure. 10 Variation of erosion rate with impact velocity at room temperature, and elevated temperatures at 300 C and 600 C (1.25Cr-1Mo-V Steel)